Continuum Monte Carlo simulation at constant pressure of stiff chain molecules at surfaces

F. M. Haas
Institut für Physik, Universität Mainz, 55099 Mainz, Germany

R. Hilfer[a)]
Institut für Physik, Universität Mainz, 55099 Mainz, Germany and Institute of Physics, University of Oslo, P.O. Box 1048, 0316 Oslo, Norway

(Received 31 August 1995; accepted 21 May 1996)

Continuum Monte Carlo simulations at constant pressure are performed on short chain molecules at surfaces. The rodlike chains, consisting of seven effective monomers, are attached at one end to a flat two dimensional substrate. It is found that the model exhibits phases similar to the liquid condensed and liquid expanded phases of Langmuir monolayers. The model is investigated here for a wide range of pressures and temperatures using a special form of constant pressure simulation compatible with the symmetry breaking during tilting transitions in the liquid condensed phases. At low pressures, the chains undergo a tilting transition exhibiting tilt directions towards nearest and also next nearest neighbors depending on temperature. At elevated temperatures and low pressure the film enters a fluidlike phase similar to the liquid expanded phase observed in experiment. © *1996 American Institute of Physics.* [S0021-9606(96)50633-1]

I. INTRODUCTION

Amphiphilic molecules, such as fatty acids ($CH_3(CH_2)_nCOOH$) or phospholipids, form monomolecular layers on water surfaces in which the hydrophilic headgroups are immersed into water while the hydrophobic alkane chains point outwards.[1] This phenomenon is utilized in the Langmuir–Blodgett coating technique, in which under suitable conditions on *p*H and temperature, monolayer or multilayer films can be transferred to a solid substrate by successively dipping the substrate into a compressed layer on a water surface. Langmuir–Blodgett films are highly ordered and their molecular ordering depends on the structure of the compressed layer on the water surface prior to dipping.[2] The ordering of Langmuir–Blodgett films plays an important role in applications ranging from microlithography and electrooptics to biochemical sensing and tribology.

Many experiments in recent years have investigated the molecular structure and phase behavior of Langmuir monolayers (see Refs. 2–5 for reviews). These studies were spurred by the possibility of combining modern x-ray diffraction methods with more traditional thermodynamic measurements.[6,7] The rodlike, but not symmetric, molecules give rise to a large variety of phases and phase transitions[4] with a rich polymorphism.

Despite differences in detail monolayers of fatty acids, phopholipids, alcohols, and esters exhibit a similar phase diagram.[8,6,5] This fact alone suggests that the structural similarities between amphiphilic molecules are responsible for the similarities observed in the phase diagrams. Hence, the chemical and atomistic differences between different molecules may not be necessary to understand the phase diagram of amphiphiles. This observation motivates our studies of highly idealized coarse grained models to elucidate the mechanisms underlying various transitions. Among these transitions, the tilting transition in the liquid condensed phases has been our main interest. We study idealized models in order to separate the influence of various coarse parameters (such as chain flexibility, symmetry of the molecules, mobility and geometry of head groups, etc.) from that of finer details (such as interaction potentials, cis-trans conformations, hydrogen atoms, etc.) on the tilting transition in these monolayers.

Given the advances in numerical simulation techniques there have already been numerous simulation studies of chemically realistic[9–19] and idealized coarse grained models[20–25] for the tilting transition in amphiphilic monolayers. Chemically realistic models with much atomistic detail have an advantage in their ability to describe dense packing effects more realistically. Molecular dynamics simulations of such models are very useful for elucidating the behavior of such models away from phase transitions. Near a phase transition Monte Carlo methods can be more efficient for obtaining the statistical averages. Highly idealized coarse grained models may be simpler (and sometimes faster) to simulate but they often suffer from neglecting some aspects of the physics. For example, treating the alkane chains as rigid cylindrical rods, originally suggested in Ref. 20, disregards the melting transition of the layer, and the intrachain conformational disorder. Such rigid rods grafted onto a triangular lattice were studied extensively in Refs. 21, 23, and 24 using continuum Monte Carlo calculations. While this model exhibits a tilting transition, it cannot show a liquid expanded phase or the restructuring and melting of the head group lattice. Although the grafting of the head groups in this model severely limits the applicability of the model to Langmuir layers the model is useful and realistic for chains that are permanently grafted to a solid substrate.[2] Chemically re-

[a)]Present address: ICA-1, Universität Stuttgart, 70569 Stuttgart, Germany.

alistic as well as coarse grained models suffer from the general limitation that the effective potentials are only inaccurately known.[26]

Layers of flexible chain molecules with mobile head groups[27,28] are intermediate between chemically realistic united atom models and idealized coarse grained models such as rigid rods or even lattice models.[25] Such models were studied in Refs. 27 and 28 using continuum Monte Carlo simulations at fixed volume. It was found that the condition of fixed volume imposes a symmetry breaking field which can suppress the restructuring of the head group lattice during the tilting transition. This was concluded from the presence of metastable boundary induced defect structures.[29] While such defects are known to exist in experiment and are, therefore, of interest in their own right,[30] they make the extraction of thermodynamic equilibrium properties from small scale simulations very difficult. Hence, it is of great interest to perform also simulations at constant pressures in which the symmetry breaking field is absent.

In the present article, we report simulations at constant pressure using an algorithm which is compatible with the symmetry breaking during tilting transitions. To facilitate comparison, we investigate a model similar to the one studied at constant area in Refs. 27 and 28. Our main objective is twofold: Firstly, we would like to confirm the existence of an expected orthorhombic distortion of the head group lattice during a tilting transition in a coarse grained model. Such observations are essential for the interpretation of constant volume simulations in which the distortion is suppressed. For example, the impossibility to distort or contract the simulation box in such simulations combined with periodic boundary conditions can lead to the appearance of negative pressures at low densities if the interaction potential has an attractive part. Secondly, we want to understand the selection mechanisms for nearest versus next nearest neighbour tilt direction and the rather high transition temperature of the first order melting transition observed in previous constant volume simulations of the same model.[27,28,31,29] In Refs. 27 and 28 the fluidized phase, appeared at temperatures roughly four times higher than the tilting transition temperature. This seems to rule out the possibility of identifying the molten state with the liquid expanded phase of Langmuir monolayers. An important result of the present study is to show that in constant pressure simulations the fluidized phase appears already at much lower temperatures.

II. MODEL DESCRIPTION

Each amphiphilic molecule is represented through a chain of seven effective monomers labeled $i=0,\ldots,6$ with $i=0$ corresponding to the hydrophilic head group of the amphiphile. The Cartesian coordinate system in three-dimensional space is chosen such that the headgroup $i=0$ is restricted to move in the $z=0$ plane representing the two-dimensional substrate. All the effective monomers are connected through a finitely extendable nonlinear elastic (FENE) potential

$$V_{\mathrm{bl}}(d)=\begin{cases} -\dfrac{c_{\mathrm{bl}}d_{\mathrm{bl}}^2}{2}\ln\left(1-\dfrac{(d-d_0)^2}{d_{\mathrm{bl}}^2}\right) & \text{for } |d-d_0|<d_{\mathrm{bl}} \\ \infty & \text{for } |d-d_0|\geqslant d_{\mathrm{bl}} \end{cases}, \quad (1)$$

where d is the distance between monomers, and $c_{\mathrm{bl}}>0$ is the spring constant. The FENE potential is harmonic at its minimum d_0 but the bonds cannot be stretched beyond a maximum length determined by d_{bl}. The stiffness of the rodlike molecules whose alkane chains are predominantly in an all trans conformation is incorporated by a bond angle potential

$$V_{\mathrm{ba}}(\theta_i)=c_{\mathrm{ba}}[1+\cos(\theta_i)], \quad (2)$$

where c_{ba} is the force constant and θ_i is the angle formed by the three monomers $i-1$, i, $i+1$. Note that V_{ba} is a three body interaction. All monomers except nearest neighbors within the same chain interact through a Lennard-Jones potential. The Lennard-Jones potential is truncated and shifted such that it vanishes at the truncation point. If ϵ is the interaction strength and σ its range then

$$V_{LJ}(d)=\begin{cases} \epsilon[(\sigma/d)^{12}-2(\sigma/d)^6-(1/d_{LJ})^{12}+2(1/d_{LJ})^6], & \text{for } d\leqslant d_{LJ}\sigma \\ 0, & \text{for } d>d_{LJ}\sigma, \end{cases} \quad (3)$$

where $d=d_{LJ}\sigma$ is the truncation point.

The model above is similar to the model used for the constant volume simulations in Refs. 27 and 28. It extends and generalizes an earlier study of a system consisting of perfectly rigid rods grafted to a hexagonal lattice and interacting with Lennard-Jones interactions.[23,24] The main difference with Refs. 27 and 28 consists in simulating at constant spreading pressure rather than constant substrate area, and in replacing the cutoff harmonic potential for the bondlengths with a FENE potential.

The earlier simulations at constant volume were found to lead to boundary induced defects.[29] These can significantly perturb the long range correlations at phase transitions. Most molecular dynamics simulations are similarly carried out at constant volume or aspect ratio of the simulation box. Simulations at constant pressure on the other hand reproduce the experimental situation more exactly, and allow the defects to relax via distortions of the head group lattice.

III. RELATION BETWEEN THE MODEL AND EXPERIMENT

The model presented in the previous section is not intended to be a chemically realistic model for Langmuir monolayers. On the contrary, we wish to study a highly idealized coarse grained model in order to understand the influence of varying degrees of idealization on the mechanisms responsible for the tilting transitions in the condensed phases. The model has resulted from previous systematic investigations of even more idealized models.[21,23–25,27,28]

Although the model is not intended to be chemically realistic it is of interest to connect the model with reality through a rough mapping of length and energy scales. Such a

rough mapping can be helpful in deciding whether the phase transitions of the model may be related to the phase transitions of the experimental system.

If a typical fatty acid with chain lengths from 12 to 30 carbons is represented by a model chain with seven effective monomers then each effective monomer of our model chains must represent roughly between two and five methyl groups. Hence, in such a mapping the diameter of the effective monomers is of order 10 Å, and the Lennard-Jones interaction range σ is of order 5 Å. For the energy scale a value for ϵ of order 200 K is a very rough estimate.

The simple attachment of the head groups to the substrate represents an important overidealization of our model. Experimentally the form and interactions of the head groups appear to play an important role. While our model is more realistic than fully discrete lattice models,[25] it contains less chemical detail than united atom models which have been investigated using molecular dynamics simulations.[9,13,15] The main difference is that our molecules are axially symmetric while the zigzag structure of united atom models destroys this symmetry. Consequently, we do not expect the model to reproduce phases associated with a herringbone ordering. We feel, however, that our model while neglecting these features represents a good compromise between computational efficiency and chemical realism.

IV. SIMULATION DETAILS

Lengths and energies in our simulations will be measured in dimensionless units defined by setting $\sigma=1$ and $\epsilon=1$. In these units the other parameters for the simulations are chosen as $d_0=0.7$, $d_{\mathrm{bl}}=0.2$, $d_{LJ}=2.0$, and $c_{\mathrm{bl}}=100$, $c_{\mathrm{ba}}=10$ which ensures that the chains do not intersect. The choice $c_{\mathrm{bl}}, c_{\mathrm{ba}} \gg \epsilon$ produces stiff rodlike chains. The system, consisting of 144 chain molecules, is confined to an area of sidelengths L_x, L_y in the $z=0$ plane. The height of the simulation box $L_z \gg 6d_0$ is chosen much larger than the length of the chain molecules.

A simplified groundstate analysis of the model was performed previously.[27,28,31] It predicts a tilting transition between a tilted and an untilted state, and highlights the importance of packing effects.

The continuum model is simulated in a canonical ensemble in which temperature, spreading pressure and particle number are kept constant. The simulation is carried out using a Metropolis Monte Carlo procedure in which individual monomer positions and the area $A=L_xL_y$ of the simulation box are updated in continuous space. The continuous position space requires to use methods adapted from molecular dynamics simulations for evaluating the interaction energies. The maximal jump distance of monomers in a single move is chosen to optimize the acceptance rate while ensuring that the chains cannot cross each other. The cutoff in the interaction potentials allows us to use an adaptation of the link cell algorithm to keep track of interacting neighboring monomers. The simulation box is subdivided into cells of sidelength larger than or equal to the interaction radius. Particles in a subcell can only interact with particles in neighboring cells. The cell contents are stored using specially designed linked pointer lists. The algorithm was developed and tested for constant volume simulations,[32,27,28] and its speed depends strongly on the density and the interaction ranges.

The partition function $Z_{N\Pi_A T}$ of the isobaric ensemble is obtained from the isochoric partition function Z_{NAT} through Laplace transformation. Denoting the surface area by A and the spreading pressure by Π_A it reads

$$Z_{N\Pi_A T}=\int_0^\infty \int \exp\{-\beta[\Pi_A A+V(\mathbf{r})]\}d\mathbf{r}\, dA, \tag{4}$$

where $\beta=1/(k_BT)$, k_B is the Boltzmann constant, $d\mathbf{r}$ is the integral of all coordinates, and all constant prefactors have been suppressed. Expectation values for an observable $X(\mathbf{r})$ in this ensemble are calculated as

$$\langle X\rangle=\frac{1}{Z_{N\Pi_A T}}\int_0^\infty \int X(\mathbf{s})\exp\{-\beta[V(\mathbf{s})+\Pi_A A] + N\ \ln A\}d\mathbf{s}\, dA \tag{5}$$

in terms of the scaled coordinates $\mathbf{s}=(r_x/L_x, r_y/L_y, r_z)$ of all the particles. The expectation values can be calculated with the usual Metropolis scheme by introducing an effective Hamiltonian

$$H_{\mathrm{eff}}(\mathbf{s},L_x,L_y)=V(\mathbf{s})+\Pi_A L_xL_y-Nk_BT\ \ln(L_xL_y) \tag{6}$$

containing two additional degrees of freedom L_x and L_y. Attempts to change the area $A=L_xL_y$ of the simulation box are carried out after each Monte Carlo step (1 MCS=1 update/monomer) of regular coordinate updates. A maximal step size of $\Delta L_x=\Delta L_y=\pm 0.01$ for the area moves was found to yield optimal acceptance rates for the chosen system size. The evaluation of the energy difference $\Delta V(\mathbf{s})$ for an area move involves a recalculation of all particle interaction potentials because the coordinates are rescaled differently in the x- and y-directions. This makes area moves computationally expensive and leads to a deceleration of the constant pressure algorithm by a factor of roughly two compared with constant area simulations.

The simulations are started from an untilted configuration of 12×12 chain molecules. The chains are positioned on a triangular lattice and directed perpendicular to the substrate. If a tilted initial configuration with hexagonal headgroup lattice is used at low temperatures the system was found to evolve into metastable states with lifetimes well beyond 10^4 Monte Carlo steps. In all simulations, periodic boundary conditions are applied in the xy directions. In each run, the system was first equilibrated for 20 000 Monte Carlo steps (updates per monomer). Subsequently averages were recorded every 500th MCS over a period of 50 000 MCS. These calculations consumed several 100 h of CPU time on IBM RS6000 370 equipment.

The two-dimensional pressure tensor was estimated from the forces on each particle using the virial theorem and the minimum image convention appropriate for periodic boundary conditions.[33] While the contribution from the bondlength and Lennard-Jones interactions to the pressure can be ob-

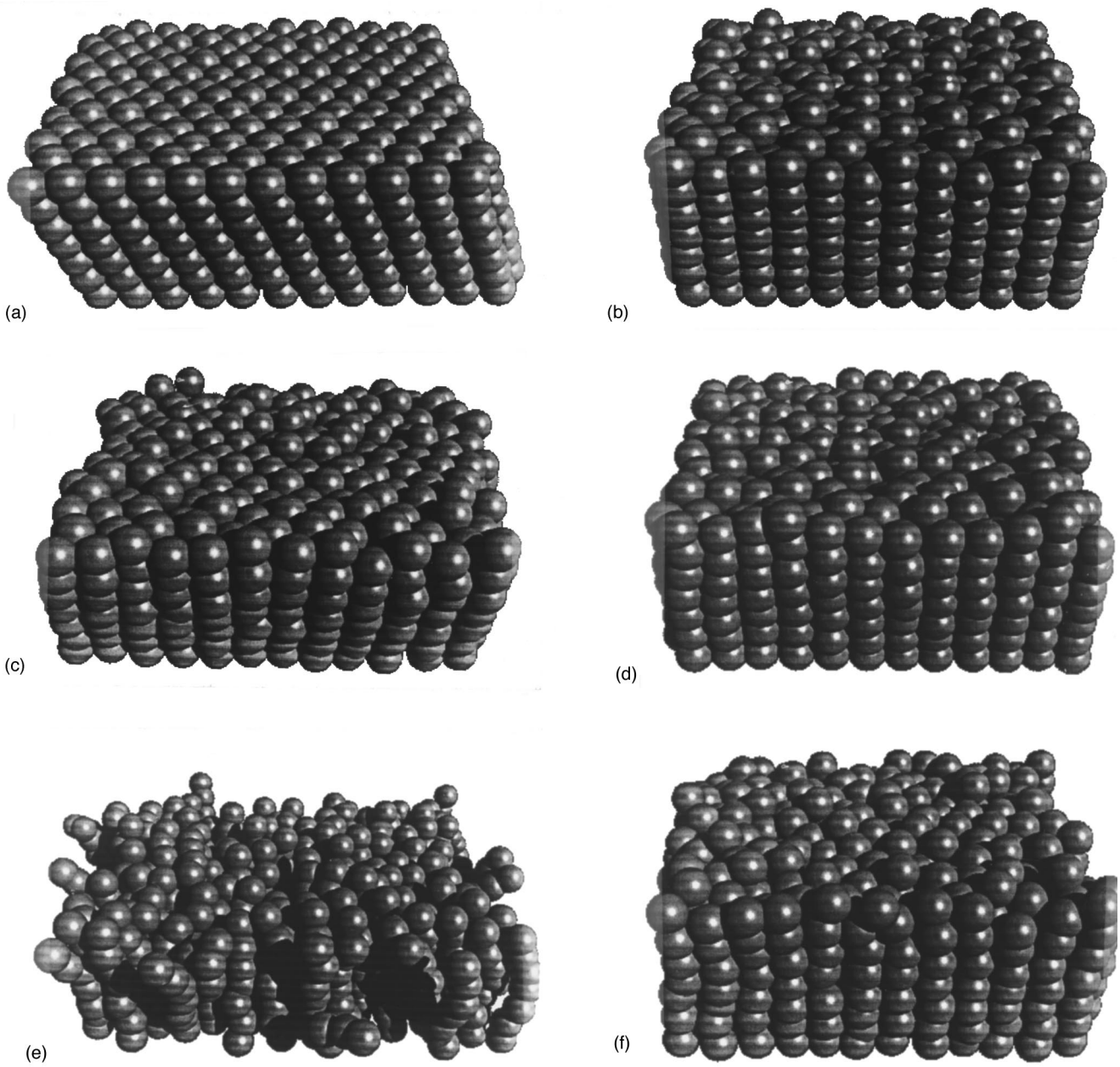

FIG. 1. Snapshots of equilibrated configurations containing 144 molecules at various temperatures and spreading pressures corresponding to (a) $T=0.2$, $\Pi_A=10$; (b) $T=0.2$, $\Pi_A=100$; (c) $T=1.0$, $\Pi_A=10$; (d) $T=1.0$, $\Pi_A=100$; (e) $T=2.0$, $\Pi_A=10$; (f) $T=2.0$, $\Pi_A=100$.

tained as usual, the contribution from the three body bond angle interaction V_{ba} has to be considered separately. It is found that the contribution of the bond angle interaction V_{ba} can be neglected.

V. RESULTS

At low temperatures, $T=0.2$, the sidelengths L_x,L_y fluctuate very little, and the system organizes itself into a configuration consisting of 12 rows and 12 columns of chain molecules. At $T=2.0$, the sidelengths fluctuate more strongly, and these fluctuations are anticorrelated in time. Increases in L_x are accompanied by decreasing L_y and vice versa yielding roughly constant area A. In general, the measured pressure agrees well with the applied pressure. Small deviations are attributed to finite size effects, and the fact that the pressure is measured from the virial theorem rather than from the free energy.

Figure 1 shows snapshots of equilibrated configurations of 144 chains at temperatures $T=0.2$, 1.0, 2.0 and pressures $\Pi_A=10$, 100. Each effective monomer is represented as a sphere of radius $\sigma/2$. At high pressures $\Pi_A=100$ the chains are compressed into a hexagonal arrangement in which all chains stand perpendicular to the substrate. At the low temperature $T=0.2$ and high pressure, the monolayer surface shows a nearly regular modulation resulting from extension and contraction of the chains along the molecular axis. At higher temperatures the surface is rough. At low pressures, the chains assume a uniformly tilted crystalline arrangement

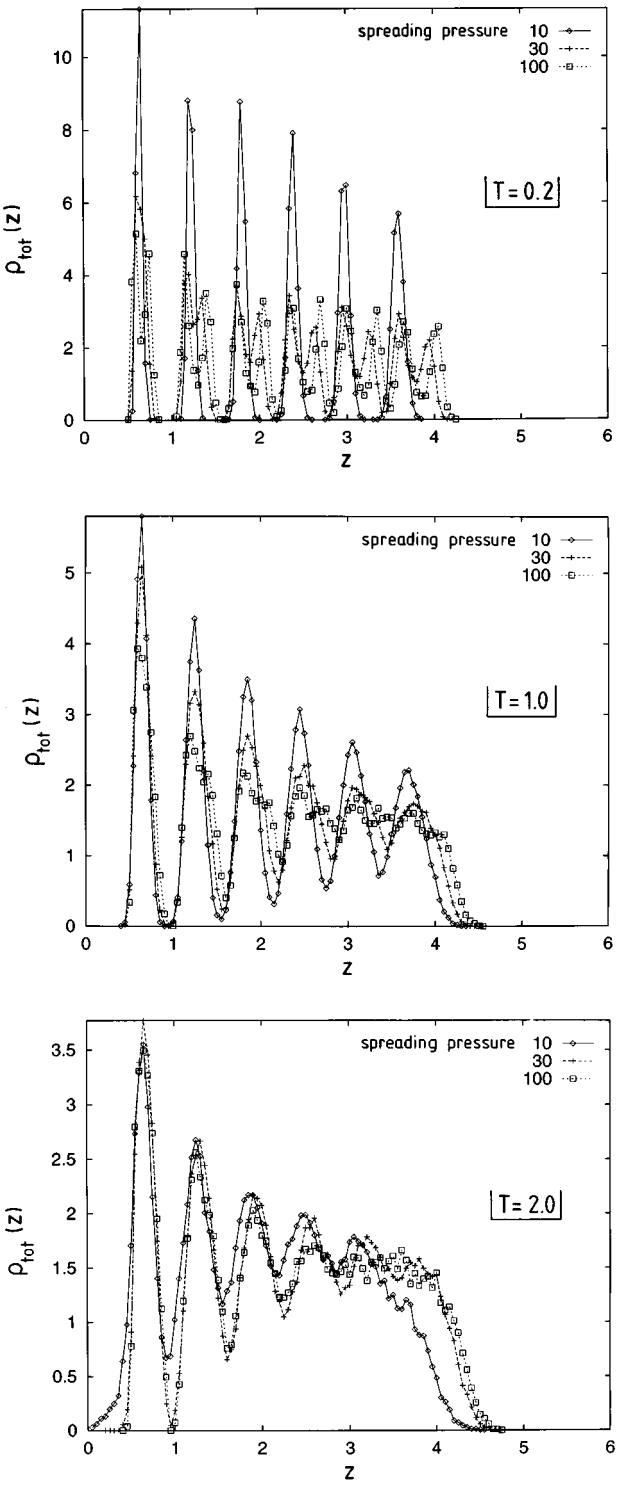

FIG. 2. Total monomer density profiles as a function of the distance z from the substrate. The densities are normalized to 6. The head group monomer ($i=0$) at $z=0$ is not included in the plot.

which progressively disorders as the temperature is increased. At $T=2.0$, the layer has molten into a fluidlike phase.

The crystalline order and the melting of the surface layer can be seen from Fig. 2 showing the density profiles along the z direction. Figure 2 also shows results at an intermediate pressure $\Pi_A=30$. At low temperature, $T=0.2$, the system is crystalline. For $\Pi_A=10$ (and $T=0.2$), there are six pronounced maxima in the density profile. The position of the last maximum corresponding to the tail group $i=6$ is significantly shifted from the value $6d_0=4.2$ corresponding to untilted chains. This indicates that the chains are tilted. At higher pressures, $\Pi_A=30$ and $\Pi_A=100$ (and low temperatures $T=0.2$), the density profile exhibits 11, respectively, 12 maxima instead of 6. This fact together with the positions of the maxima shows that the chains are alternatingly stretched and contracted along the molecular axis. The concomitant doubling of the number of monomer layers has also been observed in simulations at constant volume when the density becomes as high as 1.3.[29,31] At the intermediate temperature, $T=1.0$ and $\Pi_A=10$, the crystalline order is stabilized by the tilt order. For $\Pi_A=30$ and $\Pi_A=100$, the surface layer is beginning to melt. At $T=2.0$, the tail group layer ($i=6$) is molten for all pressures but the layered structure is still intact in the lower layers. Note, however, that for $T=2.0$ and $\Pi_A=10$, the second layer ($i=1$) is spreading into the substrate surface ($z=0$) indicating a melting of the head group lattice.

TABLE I. Monolayer thickness for different temperatures and pressures.

	$\Pi_A=10$	$\Pi_A=30$	$\Pi_A=100$
$T=0.2$	3.7	4.0	4.1
$T=1.0$	3.9	4.1	4.2
$T=2.0$	3.9	4.2	4.3

Defining the monolayer thickness from the largest (rightmost) inflection point along the density profile allows to analyze the change in monolayer thickness as a function of temperature and pressure. The results are collected in Table I. As expected, the thickness increases with increasing temperature and with increasing spreading pressure.

To analyze the tilt order we display in Fig. 3, the Voronoi diagrams for the configurations shown above in Fig. 1. In these figures, each chain molecule is shown as a dot with a short line attached to it. The dot represents the center of the head group, and the short line represents the projection of the head to tail vector into the substrate plane. In addition, the Voronoi cells are drawn around each head group to visualize the degree of crystallinity in the head group lattice. These figures show that at high pressures $\Pi_A=100$ the chain molecules are untilted at all temperatures, although defects and randomly oriented projections of small magnitude are visible at elevated temperatures. At $\Pi_A=100$, the head group lattice is crystalline at all temperatures. At low pressure and low temperature ($\Pi_A=10$, $T=0.2$), the figure shows tilting in agreement with the density profiles. The tilt is directed towards the nearest neighbor molecule. At $\Pi_A=10$, $T=1.0$, however, the average tilt direction is towards next nearest neighbors. Both of these tilt directions have been observed in experiment.[4] At high temperatures ($\Pi_A=10$, $T=2.0$), both the tilt order and the crystalline ordering of the head groups are destroyed.

The expected magnitude of the absolute value of the tilt

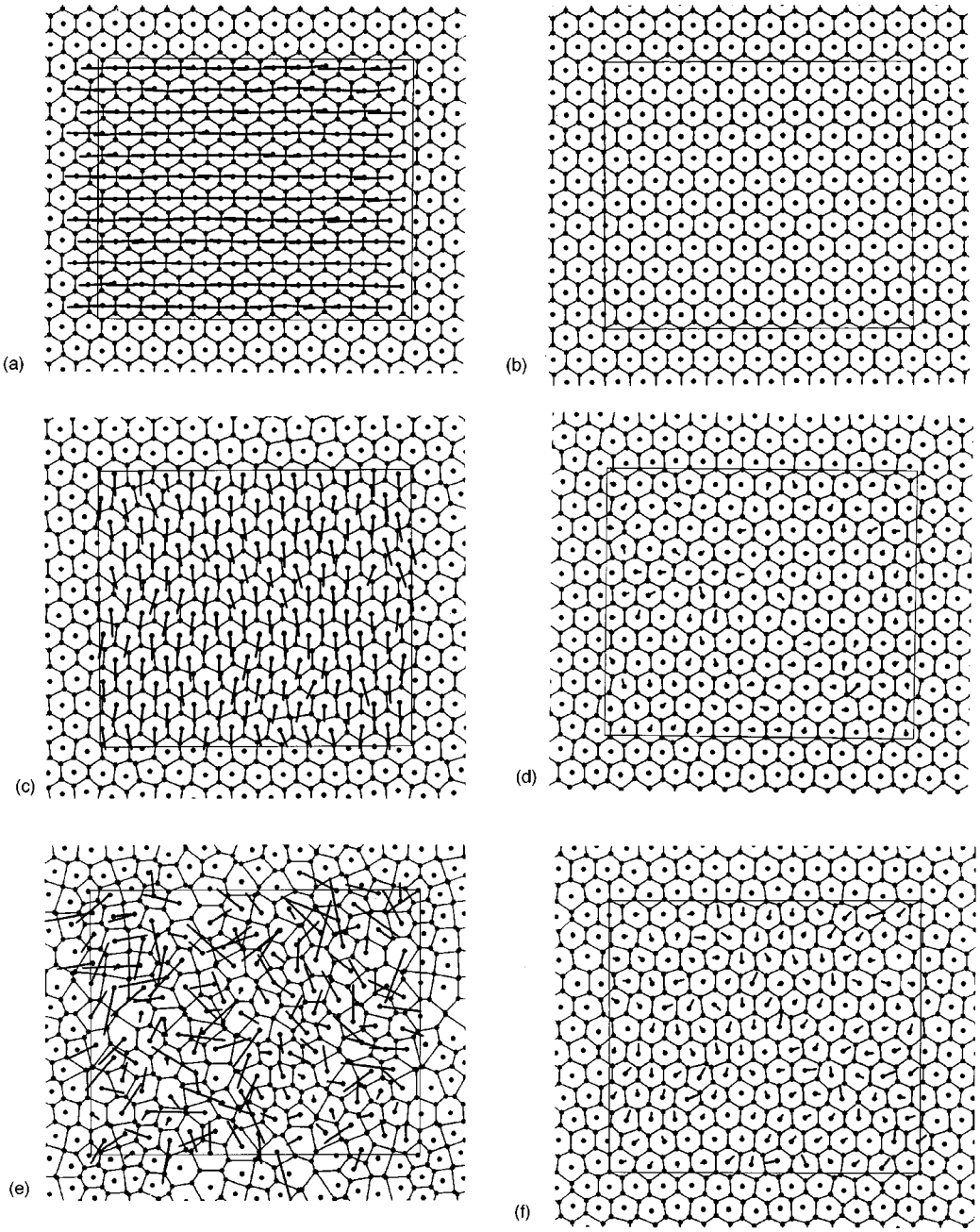

FIG. 3. Voronoi diagrams of equilibrated configurations shown in Fig. 1 at various temperatures and spreading pressures corresponding to (a) $T=0.2$, $\Pi_A=10$; (b) $T=0.2$, $\Pi_A=100$; (c) $T=1.0$, $\Pi_A=10$; (d) $T=1.0$, $\Pi_A=100$; (e) $T=2.0$, $\Pi_A=10$; (f) $T=2.0$, $\Pi_A=100$. The corresponding box dimensions are $L_x(T=0.2,\ \Pi_A=10)=11.87$, $L_y(T=0.2,\ \Pi_A=10)=9.82$, $L_x(T=0.2,\ \Pi_A=100)=10.92$, $L_y(T=0.2,\ \Pi_A=100)=9.45$, $L_x(T=1.0,\ \Pi_A=10)=11.58$, $L_y(T=1.0,\ \Pi_A=10)=10.21$, $L_x(T=1.0,\ \Pi_A=100)=11.15$, $L_y(T=1.0,\ \Pi_A=100)=9.63$, $L_x(T=2.0,\ \Pi_A=10)=14.49$, $L_y(T=2.0,\ \Pi_A=10)=11.61$, $L_x(T=2.0,\ \Pi_A=100)=11.38$, and $L_y(T=2.0,\ \Pi_A=100)=9.93$.

angle $\langle|\theta|\rangle$, defined as the angle between the end-end vector and the surface normal, is displayed over a wide pressure range in Fig. 4 for the temperatures $T=0.2$, 1.0, 2.0. At all temperatures, the tilt angle increases as the spreading pressure is lowered. However, such an increase does not necessarily indicate a larger collective tilt.[23,24,27,28] An increase in tilt magnitude can also be caused by an increase in the fluctuations of the tilt angle. The two situations can be distinguished by measuring additional quantities. The projection R_{xy} of the end-end vector $\mathbf{e}=(e_x,e_y,e_z)$ into the xy-plane is defined as

$$R_{xy}=\sqrt{\langle(\overline{e_x}^2+\overline{e_y}^2)\rangle}, \tag{7}$$

where $\overline{e_x}$ and $\overline{e_y}$ are the configuration averages of the x and y components of the end-end vector $\mathbf{e}$. The quantity R_{xy} is independent of the tilt direction. Figure 5, which shows R_{xy} over the same pressure range as the tilt angle, indicates that

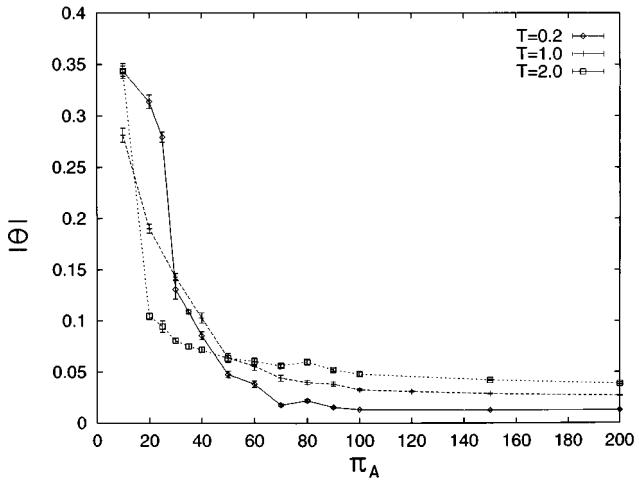

FIG. 4. Average tilt angle $\langle|\theta|\rangle$ as function of spreading pressure for temperatures $T=0.2$, 1.0, 2.0.

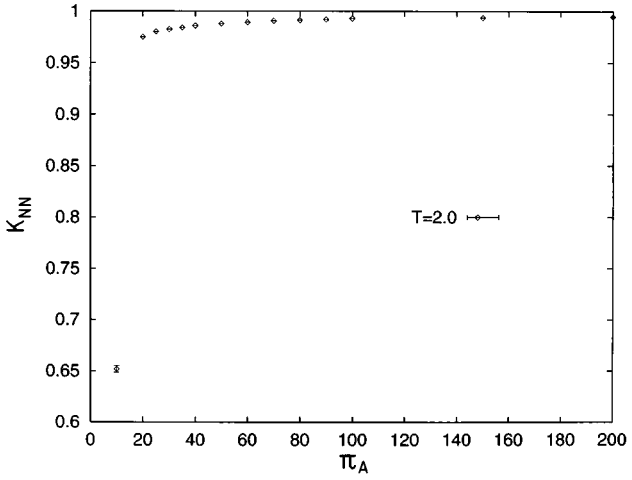

FIG. 6. Orientational correlation K_{NN} between neighboring chains as function of spreading pressure for $T=2.0$.

the jump in $\langle|\theta|\rangle$ at low pressures has different origins for $T=0.2$ and $T=2.0$. For $T=0.2$, the simultaneous increase in R_{xy} indicates a tilting transition around $\Pi_A \approx 30$. The smooth behavior of R_{xy} for $T=2.0$ indicates that the jump in $\langle|\theta|\rangle$ at this temperature is not caused by tilting but by melting. This interpretation is suggested also by the analysis of the configurations and density profiles shown in Figs. 1–3. It is further corroborated by measuring the orientational correlations between neighboring chains. The orientational correlations are measured through the quantity

$$K_{NN}=\left\langle \tfrac{1}{6} \sum \ \tfrac{1}{2}\,(3\cos^2(\theta_{NN}-1)\right\rangle, \tag{8}$$

where θ_{NN} is the angle between the end-end vectors of two nearest neighbor chains, and the sum extends over all nearest neighbor chains of a given chain. The nearest neighbor chains are defined as those six chains whose head groups have the smallest distances from the given chain. Due to steric hindrances the correlation K_{NN} is usually very strong. Figure 6 shows the pressure dependence of K_{NN} at $T=2.0$ which exhibits a sharp drop at low pressures. The same curves for $T=0.2$ and $T=1.0$ are indistinguishable from the line at $K_{NN}=1$. The sharp drop in Fig. 6 indicates the presence of a melting transition as suggested by the jump in $\langle|\theta|\rangle$ at the same pressures.

The melting transition at $T=2.0$ and low pressures appears also when plotting the specific area L_xL_y/N $(N=144)$ or the ratio of sidelengths L_x/L_y as a function of pressure as shown in Fig. 7. The area per molecule shows a steady increase from values around 0.72 to 0.93 and then a sudden jump to a value close to 1.2.

At low temperatures $T=0.2$, the specific area shows a sudden increase at the critical pressure $\Pi_A \approx 30$ for the tilting transition. This increase is associated with a similar increase in the ratio L_x/L_y reflecting an orthorhombic distortion of the head group lattice during the tilting transition. At high pressures, the ratio L_x/L_y approaches the value $2/\sqrt{3}$ for the hexagonal lattice independent of temperature.

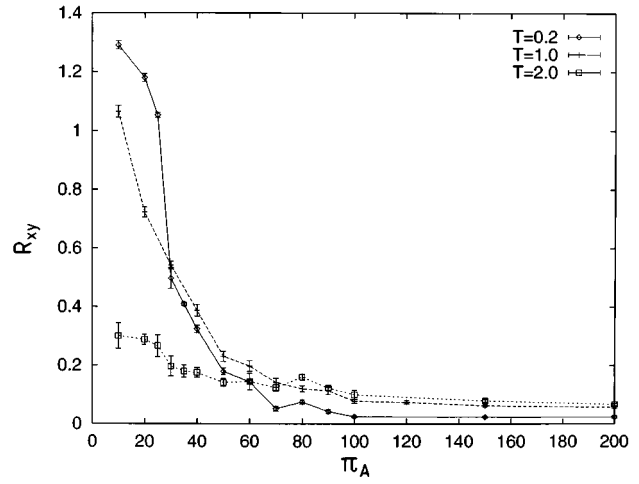

FIG. 5. Averaged projection R_{xy} of the end-end vector into the substrate plane as function of spreading pressure for temperatures $T=0.2,1.0,2.0$.

VI. DISCUSSION

Our present simulation results combined with previous simulations at constant area[27,28,31,29] indicate that the idealized coarse grained model has at least four distinct phases: an ordered phase without tilt, two ordered phases with tilt towards nearest and next nearest neighbors, respectively, and a highly disordered fluidized phase.

At sufficiently high pressures, the chains organize into a hexagonally ordered condensed phase without tilt. This phase persists throughout the whole investigated temperature range, and it can be understood as a close packing configuration. As the pressure is increased, the individual monomers begin to move away from the minima in the bond angle potentials, and this leads to stretching and contraction of the chains along their molecular axis resulting in the visible periodic modulation of the free surface. The modulation of the

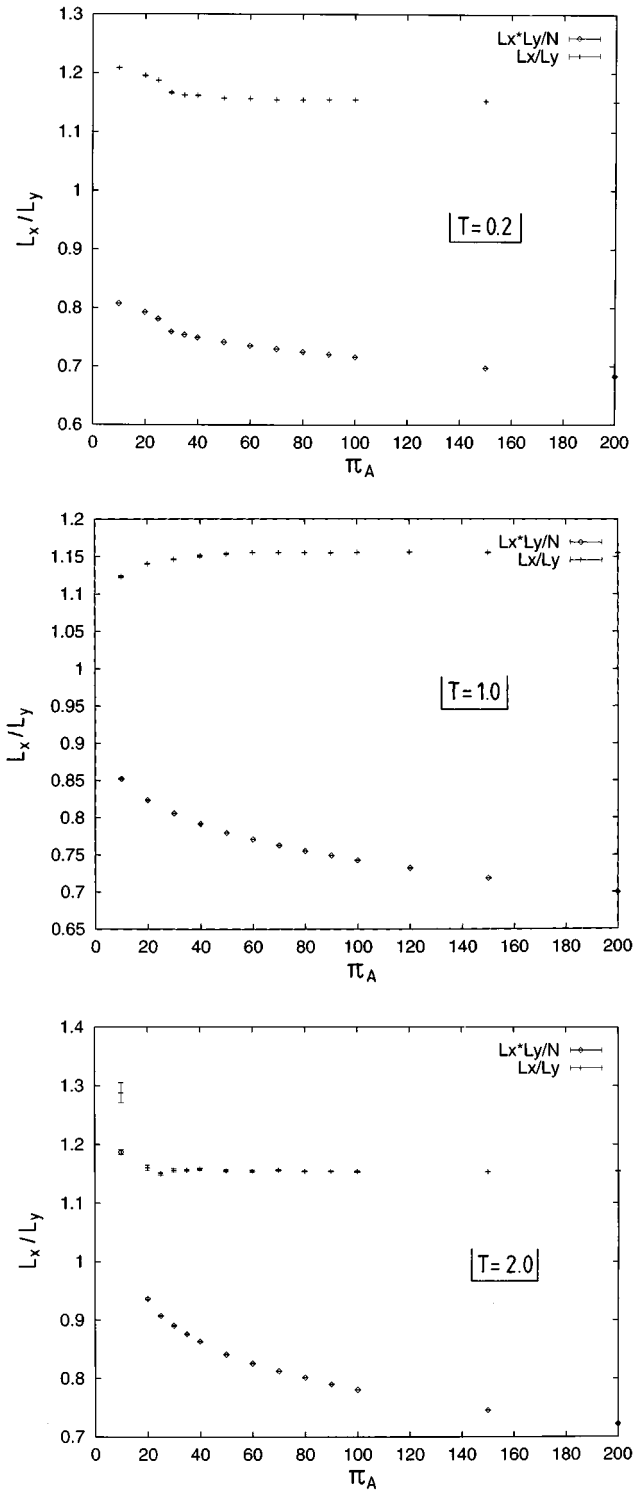

FIG. 7. Averaged specific area L_xL_y/N and sidelength ratio L_x/L_y as function of spreading pressure for $T=0.2,1.0,2.0$.

surface is expected to depend on the relative strength of the bond length potential as compared to the Lennard-Jones and the bond angle potential.

At lower pressures, the chains tilt either in the direction of the nearest neighbor chain, or in the direction of the next nearest neighbor chain. The tilting may be understood as a result of the Lennard-Jones attraction between neighboring chains. The tilt direction is the result of a complicated interplay between packing, energetic, and entropic effects. At spreading pressure, $\Pi_A=10$ and temperature $T=0.2$, we observe nearest neighbor tilt combined with a periodically modulated stretching of the chains along their axis. This indicates that packing effects are dominant for this pressure. At higher temperatures, $T=1.0$, the tilt direction changes into the energetically favored next nearest neighbor direction. A complete understanding of these effects will require not only more simulations at intermediate pressures and temperatures but in addition a systematic exploration of the space of interaction parameters which is beyond the scope of the present study.

Finally, at still higher temperatures, the individual chain conformation and the head group lattice become disordered. The system enters a fluidized phase in which more and more configurations become accessible as the temperature is increased.

A similar sequence of phases has been observed also in simulations at constant area when varying temperature and density.[27,28,31,29] Contrary to those simulations the phases appear here in a much narrower temperature range. In particular, the fluidized phase appears already at much lower temperatures than in simulations at constant area. If the rough estimate $\sigma\approx 5$ Å from Sec. III is used to map the model to experiment then the area per molecule increases from values around 23 Å/molecule to 30 Å/per molecule as seen in Fig. 7. This agrees roughly with the experimental values for the transition from liquid condensed to expanded phases, and suggests to identify the fluidized phase of our model with the liquid expanded phase in Langmuir layers.

Due to the wide range of pressures studied here the pressure resolution is poor, and, hence, our results do not allow to identify the order of this transition from the present study. Finite size scaling analyses with higher pressure and temperature resolution are needed to conclusively identify the order of this transition.

Our simulation at constant pressure using an algorithm compatible with the symmetry breaking allows to answer the questions, posed in the introduction, concerning the restructuring of the head group lattice during tilting. Figure 7 demonstrates the existence of an orthorhombic distortion of the head group lattice during the tilting transition. The magnitude of this effect may also be estimated from Fig. 7. This distortion is suppressed in simulations at constant area because the simulation box is rigid in that case. A second effect of the rigid simulation box in constant area simulations with periodic boundary conditions is the appearance of negative pressures at low densities and temperatures.[31] The negative pressure arises from the attractive part of the Lennard-Jones interactions and complicates the analysis of simulations at constant area. Our constant pressure simulations presented here are free from such complications.

In summary, we find that our coarse grained model exhibits untilted, tilted and fluidized phases similar to those observed in experiment. The model reproduces the positional ordering, bond orientational ordering and tilt ordering similar

to that observed in the condensed phases of the experiment.[6,7,4] It does not allow for herringbone ordering, however, because of the cylindrical symmetry of the chains. Our simulations at constant pressure show for the first time the experimentally known orthorhombic distortion of the head group lattice during tilting transitions in the liquid condensed phases. We have also shown that the choice of ensemble (constant pressure versus constant area) plays an important role in small scale simulations as evidenced by the large difference in transition temperatures for the appearance of the fluidized phase. This will become particularly important when trying to make quantitative predictions.

Of course, it is clear that an idealized model such as the one studied in this article can only be a small step in understanding the complexity of Langmuir monolayers, and improvements of the model are desirable in several directions. In particular, the important role played by the head groups and their interactions are inadequately represented in our model. Similarly, the cylindrical symmetry of the chains is unrealistic, as mentioned previously. Improving the model and simulation technique step by step, and studying the intermediate idealized models, it will ultimately become possible to understand quantitatively the full complexity of the phase structure observed in the experiment.

ACKNOWLEDGMENTS

We are grateful to Professor K. Binder for discussions, and we thank the Deutsche Forschungsgemeinschaft through its Graduiertenkolleg ''Physik und Chemie supramolekularer Systeme'' (F.M.H.) and Norges Forskningsrad (R.H.) for financial support.

[1] K. Blodgett and I. Langmuir, Phys. Rev. **51**, 964 (1937).
[2] C. Wöll and V. Vogel, in *Adhesion and Friction*, edited by M. Grunze and H. Kreuzer (Springer, Heidelberg, 1989), p. 17.
[3] H. Möhwald, Annu. Rev. Phys. Chem. **4**, 441 (1990).
[4] C. Knobler and R. Desai, Annu. Rev. Phys. Chem. **43**, 207 (1992).
[5] D. Andelman, F. Brochard, C. Knobler, and F. Rondelez, in *Micelles, Membranes, Microemulsions and Monolayers*, edited by M. Gelbart, A. Ben-Shaul, and D. Roux (Springer, Heidelberg, 1994), p. 559.
[6] A. Bibo, C. Knobler, and I. Peterson, J. Phys. Chem. **95**, 5591 (1991).
[7] R. Kenn *et al.*, J. Phys. Chem. **95**, 2092 (1991).
[8] A. Bibo and I. Peterson, Adv. Mater. **2**, 309 (1990).
[9] J. Harris and S. Rice, J. Chem. Phys. **89**, 5898 (1988).
[10] E. Egberts and H. Berendsen, J. Chem. Phys. **89**, 3718 (1988).
[11] J. Bareman, G. Cardini, and M. Klein, Phys. Rev. Lett. **60**, 2125 (1988).
[12] J. Hautman and M. Klein, J. Chem. Phys. **91**, 4994 (1989).
[13] J. Bareman and M. Klein, J. Phys. Chem. **94**, 5202 (1990).
[14] M. Moller, D. Tildesley, K. Kim, and N. Quirke, J. Chem. Phys. **94**, 8390 (1991).
[15] M. Bishop and J. Clarke, J. Chem. Phys. **95**, 540 (1991).
[16] S. Karaborni, S. Toxvaerd, and O. Olsen, J. Phys. Chem. **96**, 4965 (1992).
[17] N. Collazo, A. Shin, and S. Rice, J. Chem. Phys. **96**, 4735 (1992).
[18] S. Shin, N. Collazo, and S. Rice, J. Chem. Phys. **96**, 1352 (1992).
[19] H. Alper, D. Basolino, and T. Stouch, J. Chem. Phys. **98**, 9798 (1993).
[20] S. Safran, M. Robbins, and S. Garoff, Phys. Rev. A **33**, 2186 (1986).
[21] M. Kreer, K. Kremer, and K. Binder, J. Chem. Phys. **92**, 6195 (1990).
[22] M. Milik, A. Kolinski, and J. Skolnick, J. Chem. Phys. **93**, 6 (1990).
[23] M. Scheringer, R. Hilfer, and K. Binder, J. Chem. Phys. **96**, 2269 (1992).
[24] M. Kreer *et al.*, in *Computer Simulation Studies in Condensed Matter Physics IV*, edited by D. Landau, K. Mon, and H. Schüttler (Springer-Verlag, Berlin, 1993), p. 159.
[25] F. Haas, P. Lai, and K. Binder, Macromol. Chem. Theory Simul. **2**, 889 (1993).
[26] K. Binder, in *Monte Carlo and Molecular Dynamics Simulations in Polymer Science*, edited by K. Binder (Oxford University Press, New York, 1995), p. 3.
[27] F. Haas, R. Hilfer, and K. Binder, J. Chem. Phys. **102**, 2960 (1995).
[28] R. Hilfer, F. Haas, and K. Binder, Il Nuovo Cimento D **16**, 1297 (1994).
[29] F. Haas, R. Hilfer, and K. Binder, J. Phys. Chem. (to be published).
[30] T. Fischer, R. Bruinsma, and C. Knobler, Phys. Rev. E **50**, 413 (1994).
[31] F. Haas, Ph.D. thesis, Universität Mainz, 1995.
[32] R. Hilfer (unpublished).
[33] M. Allen and D. Tildesley, *Computer Simulation of Liquids* (Clarendon, Oxford, 1987).